IEEE Access
Multidisciplinary | Rapid Review | Open Access Journal

IEEE POWER & ENERGY SOCIETY SECTION

Received 12 June 2023, accepted 4 July 2023, date of publication 10 July 2023, date of current version 20 July 2023.

Digital Object Identifier 10.1109/ACCESS.2023.3293531

RESEARCH ARTICLE

Analysis of Lightning Transient Characteristics of Short-Length Mixed MMC-MVDC Transmission System

MUHAMMAD USMAN[1], KYU-HOON PARK[1], (Student Member, IEEE), AND BANG-WOOK LEE[2], (Senior Member, IEEE)

[1]HVDC Electric Power Laboratory, Department of Electrical and Electronic Engineering, Hanyang University, Ansan 15588, South Korea
[2]Division of Electrical Engineering, Hanyang University, Ansan 15588, South Korea

Corresponding author: Bang-Wook Lee (bangwook@hanyang.ac.kr)

This work was supported by the Korea Institute of Energy Technology Evaluation and Planning (KETEP) Grant funded by the Korea Government (MOTIE), DC Grid Energy Innovation Research Center, under Grant 20224000000160.

ABSTRACT Medium voltage direct current (MVDC) transmission system are growing due to their assistive quality in conventional grid and compatibility with renewable power network. MVDC distribution links with ''Mixed'' overhead (OH) & underground (UG) sections could be devised based on urban planning. UG Cables or substations are indirectly exposed to lightning strikes due to adjacent tower sections. In case of MVDC converter or cable, present researchers do not specify lightning voltage impulse level for related system voltage. Therefore, preluding electromagnetic (EM) transient investigation are required to determine the maximum lightning overvoltages for system peripherals i.e. cable & Modular Multilevel Converter (MMC) substation. This research focuses on analyzing lightning performance of OH transmission towers-cable junction & tower-substation link in case of a shielding failure (SF) and back flashover (BF) for a ±35kV short-length mixed MMC-MVDC transmission scheme. This article provides broad-band modeling method for MMC substation for lightning investigation. In addition, based on a detailed time-domain parametric evaluation in *PSCAD/EMTDC* program, lightning impulse voltage across the transmission line's pole insulator and embedded cable section are estimated along with numerical validation relying on travelling wave theory. Effect of project parameters such as tower grounding resistance, riser section surge impedance (which connects cable & OH line) and cable length on lightning overvoltage impacting the cable and connected tower section has been demonstrated.

INDEX TERMS MVDC transmission, modular multilevel converter, maximum shielding failure, insulation flashover, PSCAD/EMTDC, sheath grounding, riser section, DC cable.

I. INTRODUCTION

Commercial application of DC transmission systems has increased drastically over the past few decades. As compared to AC power systems, electronic power converters offer better integration with unconventional/low footprint power resources and more efficient power management. This has led to the construction of medium voltage DC links by energy subsidies and research consortiums across the globe [1], [2] i.e., ANGLE DC project in Europe, ±10 kV MVDC distribution project in Zhangbei, Zhuhai and Guizhou and HVDC Light (Denmark-Sweden).

As reported, most MVDC projects are point-to-point links or based on underground (UG) power cables [2], [3]. However, recent proposals for the conversion of MVAC transmission lines to DC have paved the development of mixed MVDC lines [3], [4]. These transmission corridors could pass through urban or suburban regions. Where availability of space, visual impact, and city planning could influence transmission infrastructure. Thus, MVDC projects with partial overhead (OH) and UG transmission segments would be constructed worldwide like HVDC projects. In such a

The associate editor coordinating the review of this manuscript and approving it for publication was Sinisa Djurovic.

scenario UG cable and MVDC substation are exposed to indirect lightning strike. Overvoltages caused by such events are important to be investigated for insulation coordination of cable system & substation. Consequently, lightning overvoltage on cable-overhead line (OHL) junction has been studied for MVAC system [5]. Methods to calculate lightning overvoltage surge along a DC cable in a mixed transmission system have been demonstrated in few researches [6], [7].

Currently, significant lightning research has been conducted on ''Line Commutated Converter'' (LCC) DC transmission lines at HVDC level including ''Mixed'' transmission Links [8]. Contrary to MVDC projects which are 10-100km in length, HVDC systems have long-length transmission lines thus reflection and refractions from the converter substation are not taken into consideration for lightning studies. Usually, insulation coordination of few towers and cable sections with varying length are studied [9]. Latest MVDC corridors are composed of modular multilevel converter (MMC) along with DC specialized switchgear and DC circuit breakers (CB); standards for such power projects are being evolved i.e., PROMOTioN Project in Europe. Some research articles had shed light on high-frequency MMC lightning study. Gao et al. [10] depicts MMC converter station by representing the electronic switches as open/closed switches depending on their state. A detailed model of submodule (which is building block of MMC converter) has been defined in reference [11]. This is done by representing stray capacitance and inductances in an IGBT of submodule. Zhu et al. has done a thorough electromagnetic investigation (EMI) of MMC converter station by representing the structural capacitances of submodules housed in a vertical configuration [12].

The scope of this paper is to derive lightning impulse voltage across the UG Cable, adjacent overhead transmission line (OHTL) tower's as well as DC substation in a mixed MMC-MVDC grid. In order to obtain a general statement about the occurring voltage stresses, parametric evaluation and time-domain analysis has been performed. A variety of system parameters like transmission tower grounding conditions, cable length & riser surge impedance is evaluated under shielding failure and back flashover lightning current. It is not intended to conduct entire insulation coordination studies within this research. However, compared to [5] understanding and concept about the lightning surge waveform across cable and transitioning tower insulators have been broadened for MVDC system. Additionally, modelling depth and scope regarding wide-band MMC converter & substation for lightning study has been fundamentally extended from previous research [10].

This article is further structured as follows. Section II provides a description of ±35kV Mixed symmetric monopolar MMC-VSC transmission with a brief explanation of wide-band converter station & transmission line model for lightning investigation in *PSCAD/EMTDC* program. Project specifications for transmission infrastructure from articles examining MVAC to MVDC distribution system are utilized and interpolated [7], [14]. Section III provides an overview of shielding failure (SF) and backflash-over (BF) lightning intrusion waveform for system under considered. Subsequently, a method to include steady state DC system voltage at the converter station for accurate lightning analysis is also reported. Section IV portrays a scenario in which lightning strike at a tower adjacent to cable connected transmission tower. Peak lightning transient overvoltage at various location of OHTL, riser and cable section are estimated in *PSCAD*. Furthermore, equations are formulated to validate the following contribution:

- Recognized and explained the superior flashover performance of transitioning tower under the influence of SF.
- Identified the role of tower footing resistance on farthest tower insulators' flashover.
- Investigated the variance in BF overvoltage waveform at tower insulator w.r.t pole's polarity and explained higher flashover probability of -ve/+ve pole insulator at transitioning and adjacent towers as compared to SF.
- The highest lightning peak intrusion voltage across the cable length has been estimated with regards to location & variation in length.
- Role of riser section's (which connects OH line & cable) surge impedance on lightning surge on transitioning tower have been analysed.
- Analysed the retarded surge waveform across the cable when surge arresters are installed.

Section V present lightning transient voltages across MMC converter & DC substation with following contributions:

- Analyzed the impact of length & mutual surge impedance of substation busbar on overvoltage's at converter station peripherals in case of SF & BF.
- Proved that hypothetical DC voltage source introduced in section III appropriately adds the steady-state system voltage in *PSCAD/EMTDC* for lightning studies.

Finally, section VI & VII provide a general evaluation and conclusion respectively.

II. SYSTEM MODELING AND DESCRIPTION

A. TRANSMISSION LINK PARAMETERS

A half-bridge MMC converter Monopolar ±35kV point to point link is considered for the manuscript which is connected to a 22.9kV AC system on both sides. Two 10km OHL section are connected with underground cable section in *PSCAD* model. Where sheath of the cable is solidly bonded to OHGW. Cable length is taken as variable in this study to investigate the worst-case scenario. The MMC converter station is composed of 6 arms, each comprising of 28 half-bridges. The detail of fundamental components of converter stations is given in Table. 1 along with the basic structure of the transmission structure, shown in Fig. 1.

Based on the relatively small size of the MVDC converter station as compared to higher voltage levels, the substation is considered to be confined indoors. As switchgear for DC systems are being developed isolated till now i.e., DC circuit

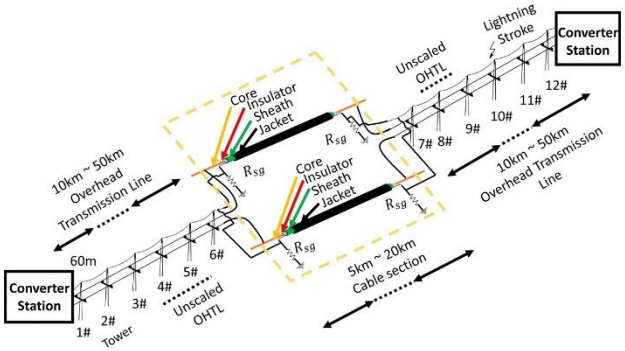

FIGURE 1. A general model of mixed MVDC point-to-point link with VSC converter station.

TABLE 1. Parameters of ±35kV MVDC transmission link.

Equipment	Converter station 1st (Master control) & 2nd (PQ control)
converter topology	Half-bridge sub-module based symmetrical monopolar configuration
power rating	34.2 MW
DC rated voltage	±35 kV
submodules per arm	28
voltage of submodule	2.5kV (max)
submodule capacitor	3.26 mF
DC nominal current	434 A
bridge arm reactor	17 mH
pole reactor	10 mH

breaker topologies devised are independently built or other disconnectors/earthing equipment are incorporated according to converter topology [15], [16]. For a short-length transmission line, one DC interrupter on each pole could be enough for current fault protection. Thus, a DCCB is installed on positive pole of one substation & negative pole of the other substation.

B. CONVERTER STATION MODELING

To evaluate the response of MMC substation under high-frequency surge, each part must be modelled appropriately. For steady state study, converter station sub-modules are represented as a voltage source with equivalent resistance [18], [19]. For any instance, during normal operation, the capacitor voltage in submodules face insignificant change as shown in Fig. 2.

Additionally, lightning surges have a very high frequency (more than 10MHz), much large than the switching frequency of converter station. Computation for such a small time period doesn't require conventional MMC converter models in *PSCAD*. Thus, voltage source in *PSCAD* with converter surge impedance is used to represent MMC for this investigation.

The MMC converter station arms are taken to be a vertical pile of connected submodules. Each submodule (SM) is in a half-bridge configuration with 2 IGBT (1200G450350) [20]. The stray capacitance & inductance of them are used to model the SM [11]. Although the submodule tower structure has no electrical connection with the MMC power-electronic

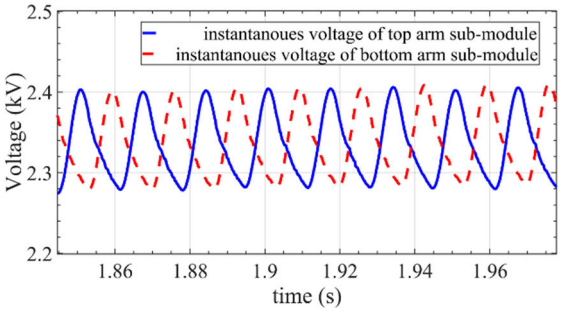

FIGURE 2. Prospect of voltage across the submodule capacitance in an arm of MMC converter.

equipment, for high surge overvoltage evaluation, the stray capacitance of the metallic MMC tower must be accounted. Zhu et al. [12] discuss a set of stray capacitances subjected to converter station. The housing capacitance between the submodules could be convolved into just two types i.e., terminal to ground and SM parallel stray capacitance (Fig. 3). For instance, $C_{(n-27)}$ and $C_{(n-28)}$ are the terminal to ground stray capacitance of sub-module 28, while C_{28} represent stray capacitor across the SM. For such structures, stray elements must be calculated exclusively. Here, 10pF is utilized for both types of SM's stray capacitances. Thus, accounting for internal & external stray elements of SM's.

C. SWITCHGEAR

The use of special type of DC interrupter in an MVDC grid is eminent for grid protection. A lot of DC CB have been proposed and evaluated but only few of them have been physically developed and tested i.e. offshore HVDC system on Nan'ao island in China [24]. A ±27kV Forced Oscillating interrupter has been developed in the PROMOTioN project [25]. The stray components of Vacuum interrupter (*VI*) and other electronic parts of that DC CB has been considered for the supposed substation. Detailed information about additional elements of DC breaker is presented in Table. 2 and Fig. 4. *VI* is in closed condition with a resistance of 80$\mu\Omega$. Wideband modelling of DC CB's surge arrester is done as explained in section VI-F.

Disconnector or breakers are required for energizing and protection of any general power network. The number and type of switchgear in a practical MVDC link could vary. Thus, derived configuration of substation is utilized [15]. Disconnecting switches and measurement transformers are represented as their parasitic ground capacitances [21], [22], [23], [24] (as depicted in Table. 3). Necessary elements like Converter Disconnector switch (CD), Pole Line Earthing switch (PLES) or Electrode Line Disconnector switch (ELD), etc. are incorporated (Fig. 5(a)). Typical Air Insulated Substation (AIS) busbar has a self-surge impedance of 350Ω [29]. To consider the effect of mutual surge impedance between busbars, they are represented as frequency-dependent line model in *PSCAD/EMTDC* [21]. Dimensions of busbar are presented in Fig. 5(b). The total length of AIS busbar is 25m per pole. Additionally, Surge retardation of 20% has been

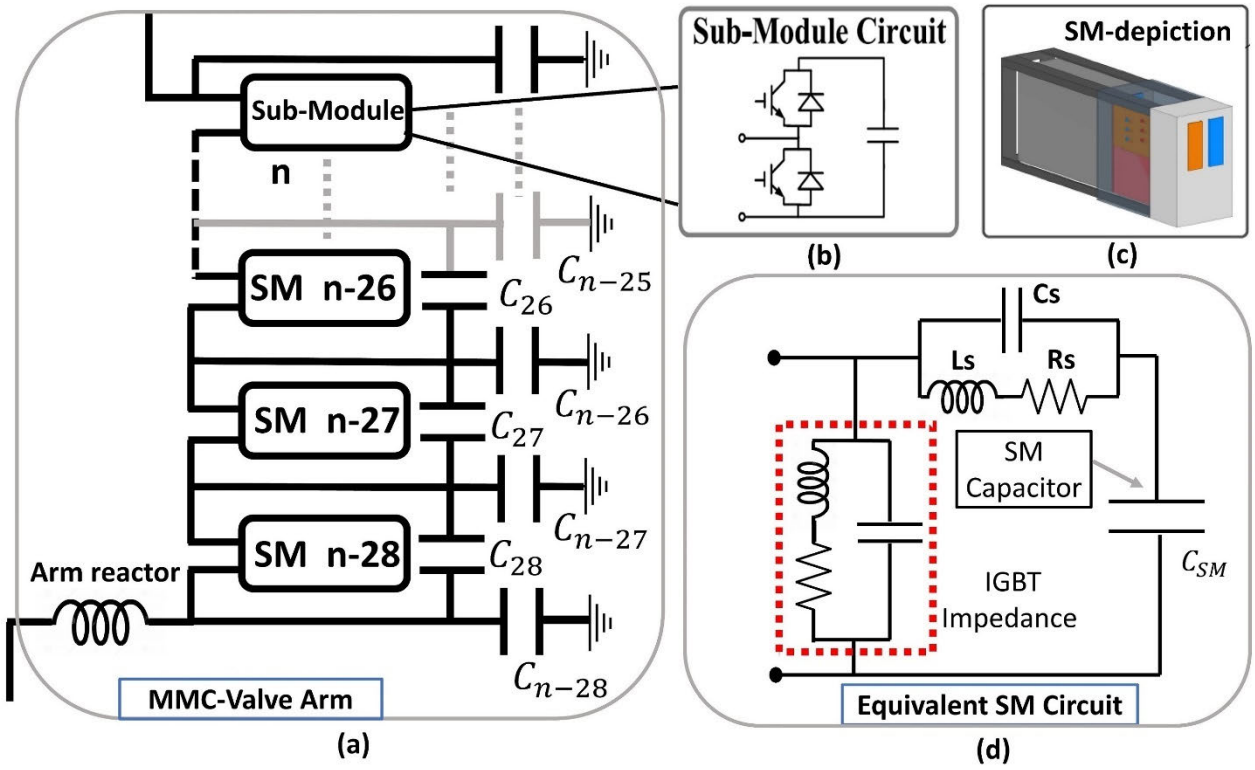

FIGURE 3. (a) High-frequency converter station infrastructure layout. (b) Basic electrical configuration of half-bridge submodule. (c) compactly enclosed MMC submodule. (d) high-frequency equivalent of internal Submodule circuit.

TABLE 2. DCCB estimated value of different elements [25].

R	C	L	R_{VI}	C_{VI}	L_{VI}	Terminal to earth capacitance (C_g)	Surge arrester Clamping voltage (SA)	Surge arrester stray capacitance (C_{SA})
50mΩ	2.5μF	19μH	50Ω	0.2nF	50nH	15pF	52kV	5.2nF

added to account the presence of bushings, supporting insulators & measurement equipment in substation. Finally, the interconnection between the transmission line and substation are modelled as lumped inductance of 4m (1μH/m) [9].

D. TOWER AND LINE STRUCTURE

For this study, experimented AC transmission equipment for DC compatibility is chosen [4]. Compact tower structure reduces carbon footprint and electrical interference in line [13]. However, audible corona and insulator flashover limits the tower compactness. For ±35kV line, the Electric field strength model of Austrian 30kV AC tower has been interpolated [4] (Fig. 6(b)), similar tower model has been utilized in other studies [26]. The considered tower is a conical 'T' shaped galvanized steel pole. The tower is grounded using a 2m lead wire with a 0.05m radius. Also, a ground wire is placed 1.545m above the pole conductors.

In *PSCAD/EMTDC* Frequency-Dependent phase model has been incorporated that can represent transmission lines over a wide range of frequencies with a DC Correction factor. The line is divided into multiple sections in *PSCAD* to

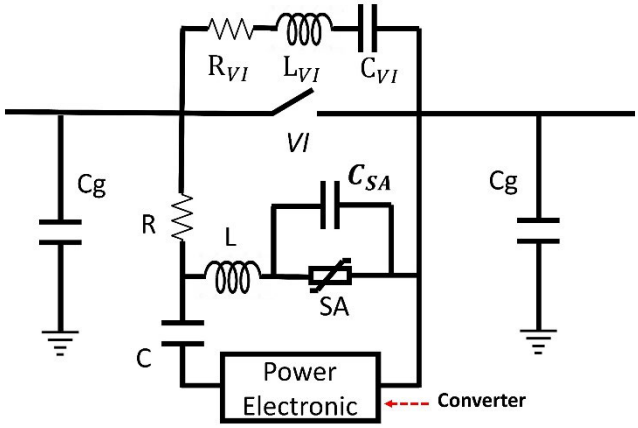

FIGURE 4. DC circuit breaker wideband model.

emulate the overvoltages midway between it. Transmission tower is simulated as Bergeron line model to represent tower surge impedance & cross arm/braces surge retardation.

Tower structure's surge impedance (Z_T) is evaluated based on its geometry. (1) & (2) are incorporated in *PSCAD* as

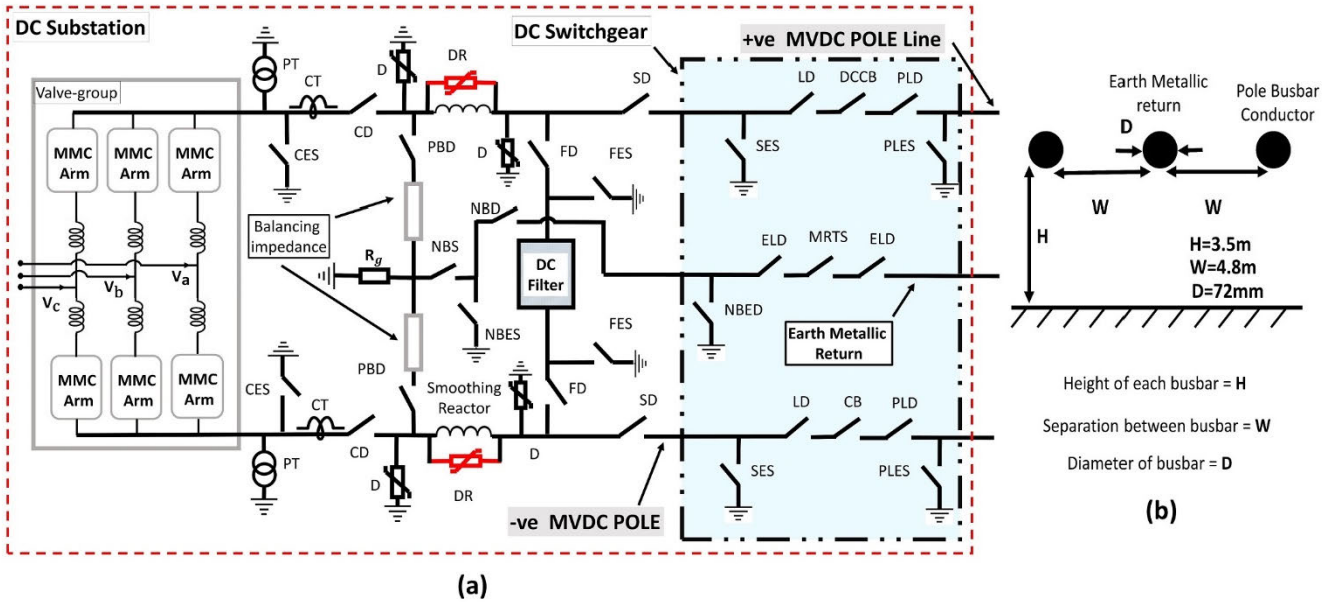

FIGURE 5. (a) MVDC substation depicting the electronic converter and switchgear. (b) Configuration and dimensions of air insulated busbar at substation.

transmission line model with 15% surge retardation [27].

$$Z_T = 60 \ln\left(\cot\frac{1}{2}\tan^{-1}\left(\frac{R_{avg}}{h_1+h_2}\right)\right). \quad (1)$$

$$R_{avg} = \frac{r_1 \times h_2 + r_2\,(h_1+h_2) + r_3 \times h_1}{h_1+h_2}. \quad (2)$$

where, R_{avg} (2) is a ratio composed of height from base to midspan of tower h1 (m) and midspan to top h2 (m), 4.5m each, while r1, r2 & r3 are the top, midsection and bottom radius of the tower structure which are 0.1m, 0.25m and 0.5m repeatedly for 9m conical tower structure [27]. Z_T calculated by this scheme is equal to 209 Ω. Short length grounding rod and tower portion between the OH power cable (PC) & ground wire (GW) are presented as RLC lumped model (for earth resistivity ρ 100 Ω.m) and inductance respectively as shown in Fig. 6(a) [22], [28].

E. INSULATOR MODELING

Pin type ceramic insulator VHD 35-G based on Austrian standards have been utilized for this study [30], DC evaluation of similar insulators has been done before [4]. For the insulator under consideration, the overall capacitance is 100pF which is installed in parallel with the ideal switch [31]. The inductance of the insulator path can be modelled as a lumped inductance (1μH/m) in series with the switch as depicted in Fig. 6(a). Although there are multiple methods to evaluate insulator flashover under the influence of fast front transients. However, for insulator of length shorter than 1.2m 'Disruptive effect method' could be utilized [32]. This technique evaluates breakdown process as a function of voltage applied across the insulator and time duration of the applied voltage.

TABLE 3. *PSCAD* representation of MMC switchgear [10], [23].

Equipment	Abbreviation	Capacitance
Converter Disconnector Switch	CD	
Substation Disconnector Switch	SD	
Line Disconnector	LD	
DC Circuit Breaker	DCCB	
Pole Line Disconnector	PLD	
Neutral Bus Switch	NBS	
Neutral Bus Disconnector	NBD	
Electrode Line Disconnector	ELD	50 pF (pole
Metallic Return Transfer Switch	MRTS	to ground)
Filter Disconnector	FD	
Converter Earthing Switch	CES	
Filter Earthing Switch	FES	
Substation Earthing Switch	SES	
Pole Line Earthing Switch	PLES	
Potential transformer	PT	100 pF
Current transformer	CT	50 pF
Smoothing/Pole reactance	--	50 pF

In case, the insulator voltage exceeds a certain value X (kV), the breakdown of air gap can be evaluated, mathematically formulated as:

$$\int_{to}^{t} \left[V_{(t)} - X\right]^K dt \geq D \quad (3)$$

where "D" is Disruption effect/Area criteria specific for a certain length of insulator. Evaluated by the integral of difference between instantaneous voltage across the insulator $V_{(t)}$ and the triggering voltage X, starting from the lightning triggering instance t_o. Once the integral value increase above D the above-mentioned ideal switch is closed in the simulation to emulate insulator flashover. The constants (X, K, D) for 0.29m long insulator are given in Table. 4 [17].

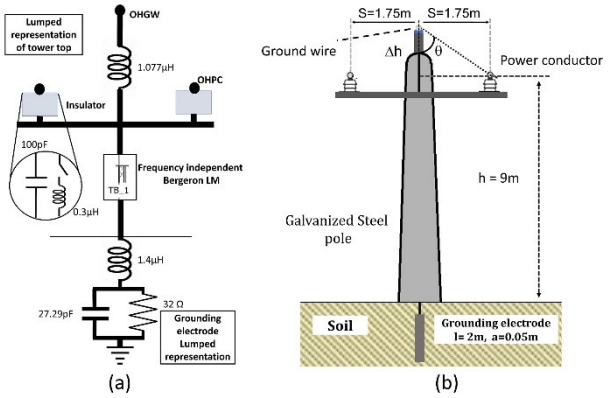

FIGURE 6. (a) High-frequency tower model. (b) Overhead ±35kV galvanized steel pole with ground wire.

TABLE 4. Disruption Effect Model Constraints for ±35kV insulator [17].

VHD 35-G height (m)	K	X (kV)	D
0.29	0.92	170	0.037

F. UNDERGROUND CABLE

Like *PSCAD* transmission line representation, the underground cable could be modelled as frequency-dependent (phase) model. The cable sections for both the poles are designed as 1-core XLPE Cable [26], 0.5m apart from each other and 1.5m deep underground. The core diameter, insulation, and sheath thickness along with the single cable depth are depicted in Fig. 7(a). The cable poles are divided into several sections to evaluate the voltage in separated sections of the cables. The lightning-withstand-level (LIWL) of cable core insulator is 170kV [33] (IEC 60071-1) that means if the cable overvoltage, due to lightning, surpasses this value the inner insulation of cable may rapture. Similarly, the cable sheath LIWL is 60kV. The sheath of cable sections can be grounded in multiple ways to reduce any stress on outer jacket of insulator under transient conditions [34]. Here, analysis is done by considering multi-terminal grounding as shown in Fig. 7(b). The sheath is grounded with 10 Ω (R_g) resistance at each subsection of the UG transmission section. However, R_g is also varied to study its impact on cable & sheath overvoltages (section IV-D).

G. OTHER TRANSMISSION EQUIPMENT

"Mixed" transmission line requires riser section (which is tower with underground cable connection) between overhead power cable (OHPC) and underground cable (Fig. 7(c)). Since there are no proper guidelines for riser section modelling. Asif et al. [8] has modelled it like an OHL (i.e., similar speed of wave propagation, geometry, and surge impedance). However, practically riser section should have a geometry transitioning from tower section to cable. For example, the separation between the poles and ground conductors reduces gradually and riser sections conductors must have an appropriate insulation jacket. This suggests that surge impedance of riser section might be approximately average of OHPC & underground cables. Thus, the impact of riser surge variation has been studied in this manuscript.

III. LIGHTNING SURGE INSTIGATION

The lightning surge waveshape impact transients on transmission equipment. For this study, CIGRE single lightning stroke is utilized with varying magnitude [22]. Lightning channel impedance of 1000 Ω and 400 Ω (Z_c) is added in *PSCAD* for SF and back flashover (BF) respectively as suggested in previous literature [35].

A. LIGHTNING SIGNAL WAVEFORM

In the presence of a ground wire, the lightning strokes reaching directly to the phase wire are relatively of lower magnitude. The first lightning stoke can be mathematically depicted as:

$$I = \begin{cases} at + \mathrm{b}t^n, & t < t_n \\ I_1 e^A - I_2 e^B, & t > t_n \end{cases} \tag{4}$$

where, at & bt^n form the front portion while $I_1 e^A$ & $I_2 e^B$ compose the tail portion of the CIGRE lightning model.

$$A = -(t - t_n/t_1) \tag{5}$$

$$B = -(t - t_n/t_2) \tag{6}$$

While t represents the instantaneous time after the initiation of lightning current. Similarly, t_f & S_m are the front time and maximum steepness of CIGRE lightning stroke. (see Fig. 8)

$$t_f = \begin{cases} 1.77I^{0.188}, 3 \le I \le 20kA \\ 0.906I^{0.411}, \qquad I > 20kA \end{cases} \tag{7}$$

$$S_m = \begin{cases} 12I^{0.171}, 3 \le I \le 20kA \\ 6.5I^{0.376}, \qquad I > 20kA \end{cases} \tag{8}$$

The maximum shielding failure lightning stroke current I_{MSF} is calculated by conducting Electro geometric modelling of the overhead transmission structure (proposed by IEEE Std. 1243) [36]. The geometric constraint of tower structure, in this paper, suggests an I_{MSF} of 10kA. Elements of I_{MSF} are tabulated in Table. 5 and depicted in Fig. 8.

Lightning strokes of higher values could strike at overhead ground wire (OHGW) causing BF. However, cumulative probability of very large magnitude is low i.e., chances of worst-case lightning amplitude of 200kA is less than 1% [36] which in case of an urban/sub-urban area might not directly strike a short length MVDC transmission system. In addition, occurrence of certain lightning impulse along an OHTL is estimated using project specific ground stroke density. Gao et al. [10] utilized 118kA BF lightning magnitude estimated for a period of 20 years based on the length & average ground lightning density (N_g). For a 35kV mixed AC transmission line a 150kA BF lightning current is chosen in [5]

TABLE 5. Parameters of considered I_{MSF} lightning current waveform.

Maximum steepness S_m (kA/μs)	Half time t_h (μs)	t_1 (μs)	t_2 (μs)	t_n (μs)	I_1 (kA)	I_2 (kA)	n	a (kA/μs)	b (kA/μs)
17.79	50	65.3369	0.0562	4.7119	10.0086	1.0086	18.0065	0.9763	3.323×10^{-12}

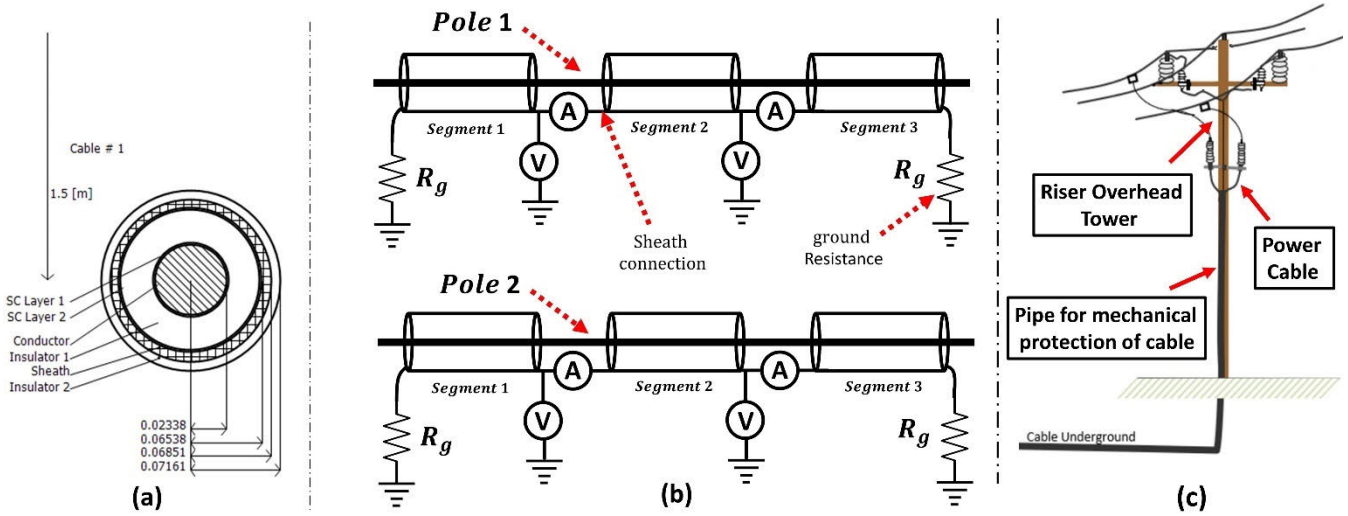

FIGURE 7. (a) Detailed cross-sectional data of a XLPE Cable. (b) Multi-terminal sheath grounding of underground transmission segment (c) riser tower & cable.

which is supposed to be rare. Here, 110kA OHGW lightning have been considered for BF analysis.

Although, for lightning insulation coordination maximum BF lightning current should be chosen based on the service life of the MVDC system peripherals i.e. cable section. However, the aim of this research is to assess the general BF lightning transients of the transmission link. Thus, a more frequent and rounded-off magnitude of 110kA has been utilized for it, which accounts for the maximum BF occurrence in a 12-year period for the OHTL tower as shown below.

Average ground lightning density (N_g) of 6.7 flashes/km^2 /year is taken here (as done in appendix of [37] for a 35kV tower).

$$N_L = \frac{N_g \left(28 \times H_T^{0.6} + W\right) \times S_f}{10} \tag{9}$$

The number of lightning strokes N_L (flashes/100 km/year) on the considered line is calculated using (9). H_T and W are the total tower height and width respectively. S_f is the shielding factor taken to be 0.5 [37]. The total exposed transmission segment is 20km (L).

$$L/100 \times N_L \times P(I) = 1/12 \tag{10}$$

$$P(i \geq I) = \frac{1}{1 + \left(I/I_f\right)^{3.4}} \tag{11}$$

(P) is a cumulative probability distribution function of lightning stroke in (10) & (11), while I_f is equal to 28.96kA. Comparing (10) & (11) indicates a maximum lightning stroke of 110kA on OHGW over a 12-year period [10].

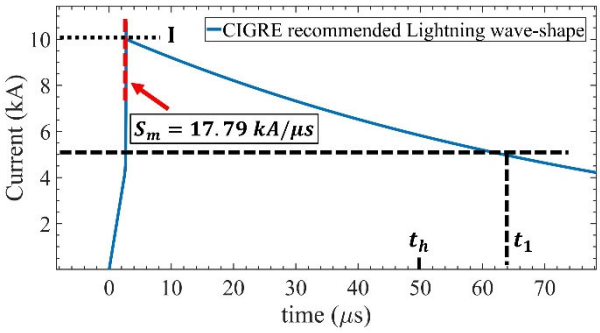

FIGURE 8. CIGRE lightning stroke with a peak amplitude (I) of 10kA.

Equation (10) has been derived in the appendix of this manuscript. Higher lightning magnitude, for example 128kA & 137kA occur once in 20 & 25 years respectively for the considered transmission line, have relatively similar maximum steepness (S_m) & front time (t_f) to 110kA lightning strike as estimated from (7) and (8). Thus, considering the random nature and relatively similar waveform of large magnitude lightning, 110kA surge can be utilized to analysis the behavior of OHTL in case of back flashover. Indirectly Induced-voltage flashovers on the transmission equipment are not studied here.

B. STEADY-STATE VOLTAGE ACROSS MVDC LINE TERMINATION

To appropriately add the DC side voltage into the system and significantly reduce any reflection from the hypothetical voltage sources, Electromagnetic wave propagation theory

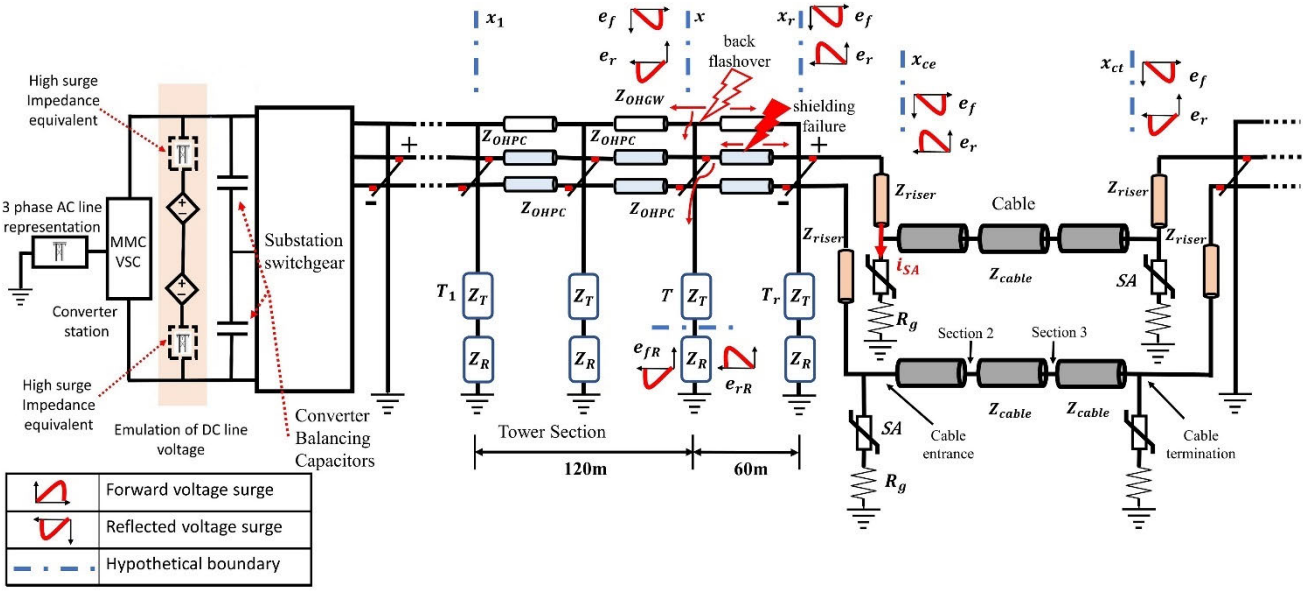

FIGURE 9. Characteristic Impedance equivalent model of considered MVDC link.

is exploited. Kirchhoff's laws are valid for characteristic impedance of any electrical system [37]. For the studied MVDC link, DC voltage source is connected in parallel configuration adjacent to one of the converter station equivalent models in *PSCAD/EMTDC*. A Bergeron lossless line with surge impedance 10 times higher than OHTL line is placed in series with voltage sources to avoid unnecessary reflection from DC source, as depicted in Fig. 9. Thus, impact of the emulated DC voltage source is negligible, and the cumulative characteristic impedance of the converter station is not impacted significantly. In addition, the reflection coefficient of the substation busbar & transmission line tends to reflect 26.06% of substation intruding surge. While the remainder of it would be refracted into the MMC substation. Reflection & transmission coefficient between substation busbar and OHPC are shown in (12) & (13) respectively [37].

$$\Gamma_{OHPC\to busbar} = (Z_{busbar} - Z_{OHPC})/(Z_{busbar} + Z_{OHPC}) \tag{12}$$

$$\Pi_{OHPC\to busbar} = 2 \times Z_{busbar}/(Z_{busbar} + Z_{OHPC}) \tag{13}$$

where, $\Gamma_{OHPC\to busbar}$ & $\Pi_{OHPC\to busbar}$ are reflection and refraction coefficient for surge transmitting from OHPC to substation. Z_{OHPC} and Z_{busbar} are the surge impedances of transmission OHPC & substation busbar in equation (12) & (13). Characteristic impedance of components of transmission link are given in Table. 6. AC line surge impedance is added at the ends to eliminate reflections from model endings.

IV. LIGHTNING STROKE ON TRANSMISSION SYSTEM

The most vulnerable sections of MVDC system from lightning overvoltage's are the line transition areas i.e., the cable section adjacent to the overhead transmission segment and the substation region [8]. Thus, lightning impact on them has been studied based on I_{MSF} (10kA) on positive power conductor and 110kA BF lightning on OHGW.

A. SHIELDING FAILURE AT OHPC ADJACENT TO CABLE

A scenario is considered where negative polarity lightning strikes a positive (+ve) polarity pole due to SF at tower (T), 60m away from the riser tower (T_r) as shown in Fig. 9. To study the influence of surge, overvoltage at four other transmission segments opposite to T_r section is considered (T_1, T_2, T_3 & T_4). Length of each (voltage measured) tower section considered is double of its predecessor i.e., T_1 is 120m away from T while T_4 is 960m.

Lightning strike will initiate a forward voltage surge (e_f) towards the cable section and reverse voltage surge (e_r) towards the transmission line/substation. Initially, total surge voltage at +ve pole of T(location x) is a sum of e_f & e_r:

$$e(x,t) = e_f(x,t) + e_r(x,t). \tag{14}$$

e_r will travel across OHPC which is connected to towers via insulators. e will result in negative voltage surge across the +ve polarity pole insulators. Meanwhile, part of the forward surge e_f will reflect from riser section x_r and remaining of it will be refracted into the cable:

$$e_r(x_r,t) = e_f(x,t)\frac{Z_{riser} - Z_{OHPC}}{Z_{riser} + Z_{OHPC}}. \tag{15}$$

$$V_T = e(x,t) + e_r(x_r,t) + e_r(x_{ce},t)\frac{2 \times Z_{OHPC}}{Z_{riser} + Z_{OHPC}}. \tag{16}$$

The reflected riser surge $e_r(x_r,t)$ will be 40% of the initial e_f value with opposite polarity as estimated from travelling wave theory [37], equipment surge impedance in Table. 6 and (15). Remaining 60% percent surge will refract towards cable entrance x_{ce}. Part of the refracted riser surge

$e_f\ (x_r, t)$ will reflect from the boundary x_{ce} and ultimately reach the impacted tower section, (depicted as third term in Eq. (16) & (17). Equation (16) shows, initially, reflected surges retards the growth of overvoltage (V_T) at +ve insulator of tower T. However, as the steeper part of the lightning surge arrives at the tower, positive insulator breaks down. Reflection from the cable end x_{ct} is not accounted for in (16) as it doesn't reach instantly due to relatively large cable length. The insulation breakdown is represented as a close switch in *PSCAD*, governed by equal area criterion model (3).

Overvoltage V_{Tn}(n = 1 to 4) at further towers opposite to riser section (T_1, T_2, T_3 & T_4) experience similar lightning overvoltages along with surge retardation due to OHTL length & towers base. This surge retardation can be accounted using attenuation constant k_n as stated in (17).

$$V_{Tn} = k_n \left[e\,(x,t) + e_f\,(x,t)\,\frac{Z_{riser} - Z_{OHPC}}{Z_{riser} + Z_{OHPC}} + e_f\,(x_r,t) \left(\frac{Z_{cable} - Z_{riser}}{Z_{cable} + Z_{riser}}\right)\left(\frac{2 \times Z_{OHPC}}{Z_{riser} + Z_{OHPC}}\right)\right]. \tag{17}$$

Fig. 10 shows the lightning overvoltage waveform across the +ve insulator of transmission towers adjacent to UG cable section due to 10kA shielding failure current at tower T. In case of T, voltage surge rises initially till 0.2μs after which reflection from riser section would dampen the voltage surge.

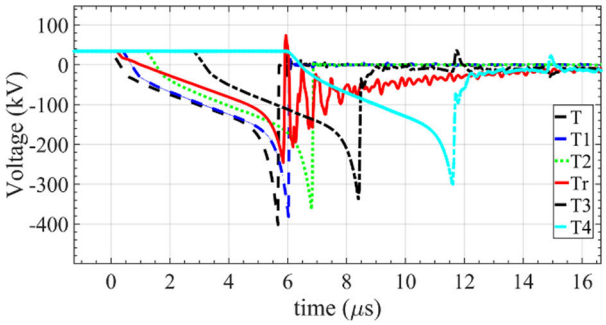

FIGURE 10. Lightning overvoltage at positive pole of adjacent tower section to the cable.

However, steeper portion of lightning surge (at 5.5μs) results in breakdown of +ve tower insulator. Fig. 11 depicts the growth of Insulation disruption coefficient of the considered tower sections insulators. Once this coefficient goes above the disruptive area criteria "D", as recommended for VHD 35-G pin type insulators in Table 4, the insulators of tower experience breakdown. In case of further tower i.e., T_3& T_4 surge retardation is imminent as expressed in (17). Due to relatively short arrival time of reverse travelling surge and smaller half time (t_h) at T_r's positive insulator, it doesn't experience breakdown.

Once the tower insulator breaks down, surge is transmitted into tower & ground. Tower surge impedance Z_T and grounding impedance Z_R is lower than OHPC this results in opposite polarity reflected wave e_{rR} to reach the tower top, retarding the further insulator surge voltage. The simulation is also done using 200 Ω.m to 800 Ω.m ground resistivity. Increment in lumped ground resistance (R_g from 64 Ω to 260 Ω) significantly raise the insulation breakdown probability on farthest towers i.e., T_3 & T_4 due to lower surge reflections from the base of adjacent towers as shown in Fig. 12.

B. LIGHTNING SURGE ON OHGW ADJACENT TO CABLE

This section discusses the backflash-over on OHTL adjacent to UG cable section. Lightning strikes the ground wire of the tower "T" for the same configuration of tower as previous section. Part of the lightning surge traverse along the impacted tower as well as forward and reverse direction on OHGW.

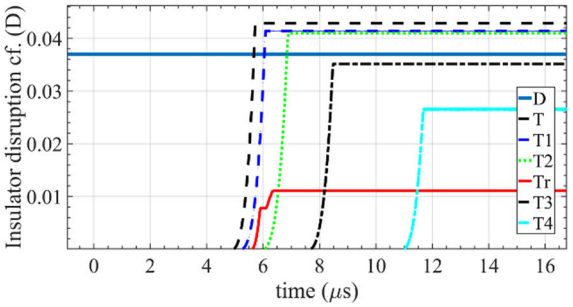

FIGURE 11. Prospect of insulation breakdown at positive pole of considered tower sections based on equal area criteria model.

It can be observed in Fig. 13 that the positive pole insulator flashover at T occurs before the negative pole under 110kA lightning impact. This is due to fact that tower insulator with opposite polarity w.r.t tower -ve polarity lightning overvoltage (U_T), experience largest voltage stress i.e., $|35kV - U_T| > |-35kV - U_T|$. Initially, the +ve insulator at T do not experience any breakdown as the surge reflected from tower base (e_{rR}) and riser/cable sheath hinders the growth of flashover until steeper portion of lightning occur at 4.5μs (Fig. 13(a)). After which +ve insulator flashover occur and part of the surge is injected into the OHPC of +ve pole which escalate as forward & reverse voltage (e_{+f} *and* e_{+r}). Part of the forward surge reflects back from the cable/ riser section to tower section. In case of negative (-ve) pole insulator, although there is surge attenuation at first due to positive pole flashover, the large surge half time (t_h), eventually leads to flashover occurring at the -ve insulator of tower T at 9.8μs. This generates a forward/reverse voltage surge (e_{-f} *and* e_{-r}) on OHPC at –ve pole.

$$V_{+Tn} = k_n \left[e_+\,(x,t) + e_{+r}\,(x_r,t) + e_{+r}\,(x_{ce},t)\,\frac{2 \times Z_{OHPC}}{Z_{riser} + Z_{OHPC}} \right] \tag{18}$$

Initially, direct OHGW surge do not cause severe tower overvoltages at adjacent tower i.e., T_1, T_2 & T_3. However, secondary negative polarity reflected surge from impacted tower (T) poles and riser/cable section arrive at insulator of

TABLE 6. Surge Characteristics of ±35kV VSC-MMC Transmission system.

Equipment	Type	Characteristic Impedance	Symbol	Wave propagation speed
Overhead power cable	147-AL1	538.8 Ω	Z_{OHPC}	2.85×10^8 m/s
Overhead ground wire	AWG (6/1) Aluminum conductor	549.5 Ω	Z_{OHGW}	2.85×10^8 m/s
Underground cable core	Single core XLPE cable (± 35)	124.2 Ω	Z_{cable}	1.75×10^8 m/s
Underground cable sheath	part of cable	23.5 Ω	--	2.02×10^8 m/s
Substation Busbar	--	316 Ω	Z_{busbar}	2.39×10^8 m/s
Hypothetical DC voltage source	--	5000 Ω	--	2.86×10^8 m/s

these tower section. Voltage surge V_{+Tn} (n = 1 to 4) at +ve insulator for adjacent tower T_1, T_2, T_3 & T_4 can be formulated as (18). Similar voltage stress could be observed on -ve pole insulators as seen in Fig. 13(b). It is seen that larger half time of CIGRE 110kA lightning strike result in longer duration of voltage surge at subsequent tower. Thus, even attenuation constant k_n, due to transmission line length, do not result in significant reduction of disruptive criterion coefficient of +ve/-ve insulator (as shown in Fig. 14), except at tower T_4. Large surge t_h also influence the surge overvoltages at riser tower T_r. The immediate reflection & refraction at T_r cause oscillations at the riser insulators but larger duration of surge result in insulator flashovers.

The maximum lightning stroke over the transmission line may vary during its service period. For instance, more frequent and less prevalent, 31kA & 200kA lightning surge may strike. Thus, these lightning strikes along with maximum lightning surge in 20 & 25 years have been studied. Fig. 15 depicts the peak overvoltages at positive pole of incident tower, and 18.75km cable entrance and ending for 31kA, 110kA, 128kA, 137kA & 200kA OHGW lightning stroke. It can be noticed that under the influence of lightning intrusion, incident tower insulator experience breakdown. However, for cable section voltage peak are higher for higher lightning current i.e., for 200kA CIGRE lightning stroke, cable entrance experiences a voltage impulse above -1000kV while for 31kA strike, its -178kV. It is expected that increase in half-time and S_m have resulted in a higher cable entrance overvoltage.

C. SHIELDING FAILURE LIGHTNING SURGE ACROSS CABLE

In case of SF, lightning surge partially refract into the cable section. Positive transmission coefficient generates negative forward voltage surge at the cable entrance which is similar in overvoltage polarity as the impacted tower. (19) represent the forward voltage surge at x_{ce} in terms of $e_f(x_r, t)$ and transmission coefficient at cable junction.

$$e_f(x_{ce}, t) = e_f(x_r, t) \frac{2 \times Z_{cable}}{Z_{riser} + Z_{cable}} \tag{19}$$

The surge $e_f(x_{ce}, t)$ travels and attenuates across the length of cable section. At cable termination x_{ct} (as depicted in fig. 9)

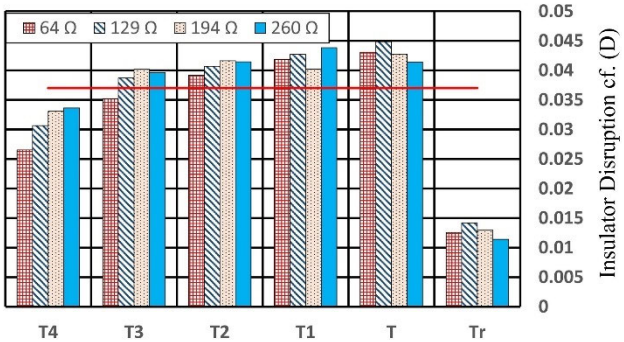

FIGURE 12. Equal area criteria coefficient at positive pole of considered tower sections w.r.t varying tower ground resistance.

a reflected backward surge is developed. Positive reflection coefficient from cable and riser junction produces backward voltage surge with same voltage polarity as $e_f(x_{ce}, t)$. Superpositioning of these multiple travelling waves might result in higher initial overvoltage at cable termination, if surge attenuation (k) of cable isn't significant as depicted in (20).

$$V_{ct} = k\, e_f(x_{ce}, t) + e_r(x_{ct}, t) + e_f(x_{ct}, t) \frac{Z_{OHPC} - Z_{riser}}{Z_{OHPC} + Z_{riser}} \tag{20}$$

For 18.75km +ve cable pole, 10kA MSF lightning overvoltages are shown in Fig. 16. The voltages at the cable entrance, entrance of sections II, III and cable termination are presented. Propagation time of cable (τ) is large as compared to lightning surge half time (t_h) thus initial surge at cable entrance subsides before any superposition occur due to reflections/refractions from cable junctions [6], [7]. As depicted in fig. 16 the first overvoltage surge at cable termination is higher than at cable entrance due to immediate constructive interference between forward and reflected waves, resulting in -205kV peak voltage surge.

D. LIGHTNING VOLTAGE AS A FUNCTION OF CABLE LENGTH

The impact of cable length on SF lightning voltage has been studied by considering varying length of the cable from 10km, 5km, 2.5km and 1.25km respectively. It is evident

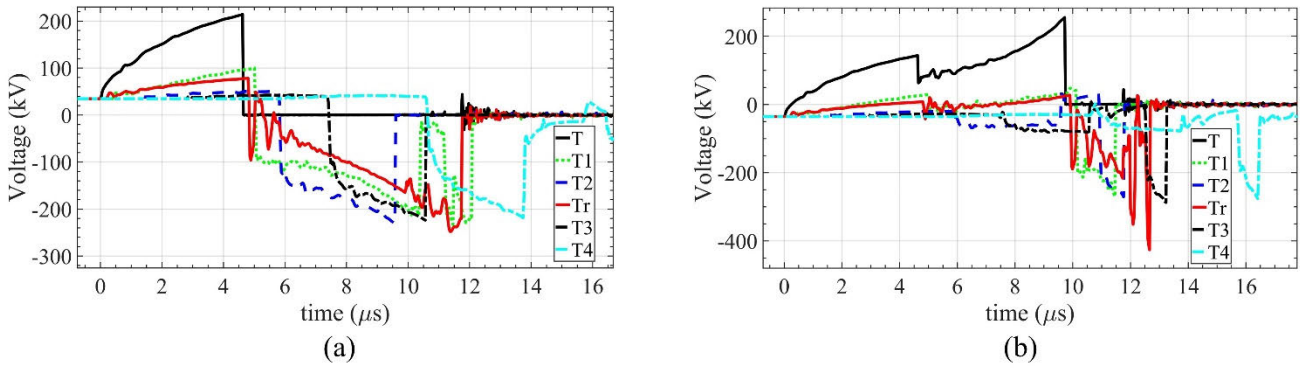

FIGURE 13. 110kA Lightning overvoltage's at tower's (a) Positive pin type insulator (b) Negative pin type insulator.

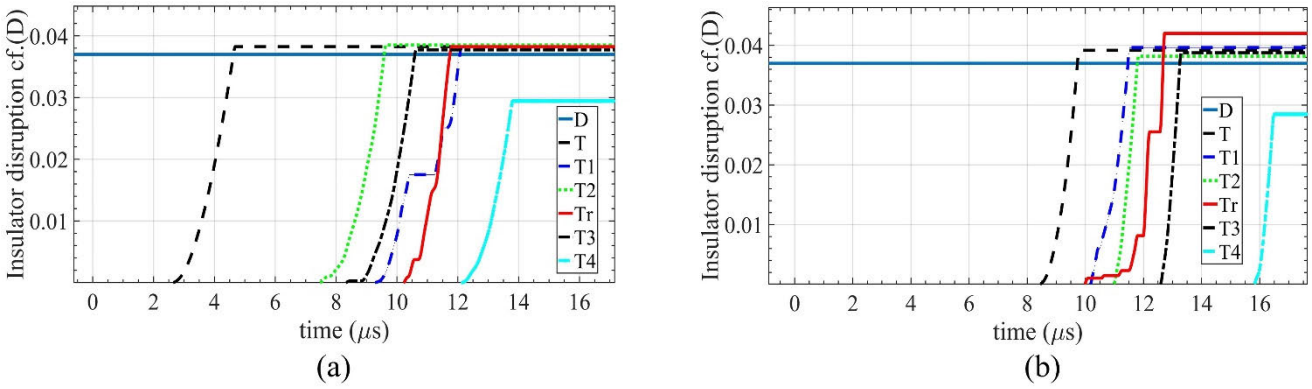

FIGURE 14. 110kA lightning flashover measurement using disruptive area criteria at tower's (a) positive pole insulator (b) Negative pole insulator.

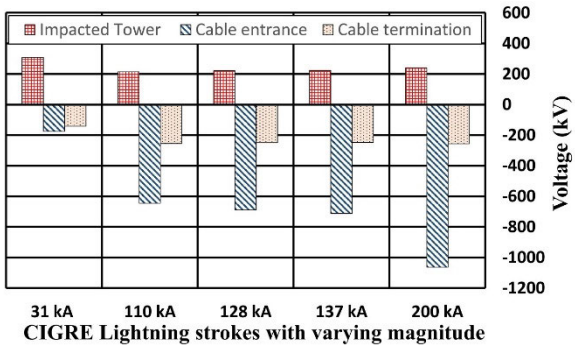

FIGURE 15. Overvoltage prospect of cable segment parts based on different lightning intrusion.

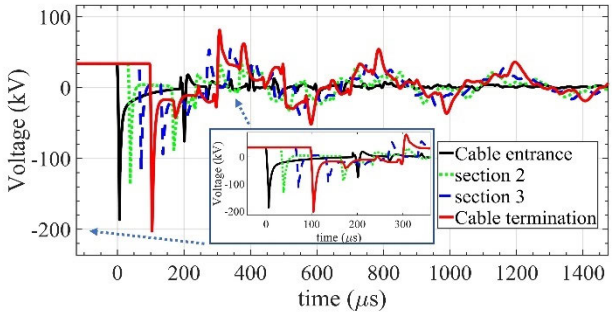

FIGURE 16. Overvoltage across an 18.75km cable segment due to 10kA surge on a 60m away tower section.

from Fig. 17 that as the length of the cable decrease (from Fig. 17 (a) to (d)) there is a significant increase in the cable termination overvoltage because a shorter cable will not dampen the surge as much as the bigger segment. This can be verified using (20) as attenuation constant (k) decrease for shorter cables. For instance, variation in cable length (from 18.75km to 1.25km) cause peak cable termination overvoltage reaches up to -300kV breaching the cable breakdown limit [33]. While peak cable entrance overvoltage remains same.

With short cables, propagation time (τ) for surge gets smaller than surge half time (t_h) which makes multiple superposition of reflected waves eminent [6], along any point of cable, before the first impulse subside i.e., for 10km cable initial lightning surge reach x_{ct} at 57.1μs as estimated using Table. 6 or depicted in fig. 17 (a). With reduced length subsequent overvoltage maxima & minima become more prominent. (See fig. 17 (c) & (d)). Cable's sheath grounding resistance may vary during its service period. It is observed that 18.75km cable entrance, under I_{MSF}, endure 6.3% increase in overvoltage when grounding resistance vary

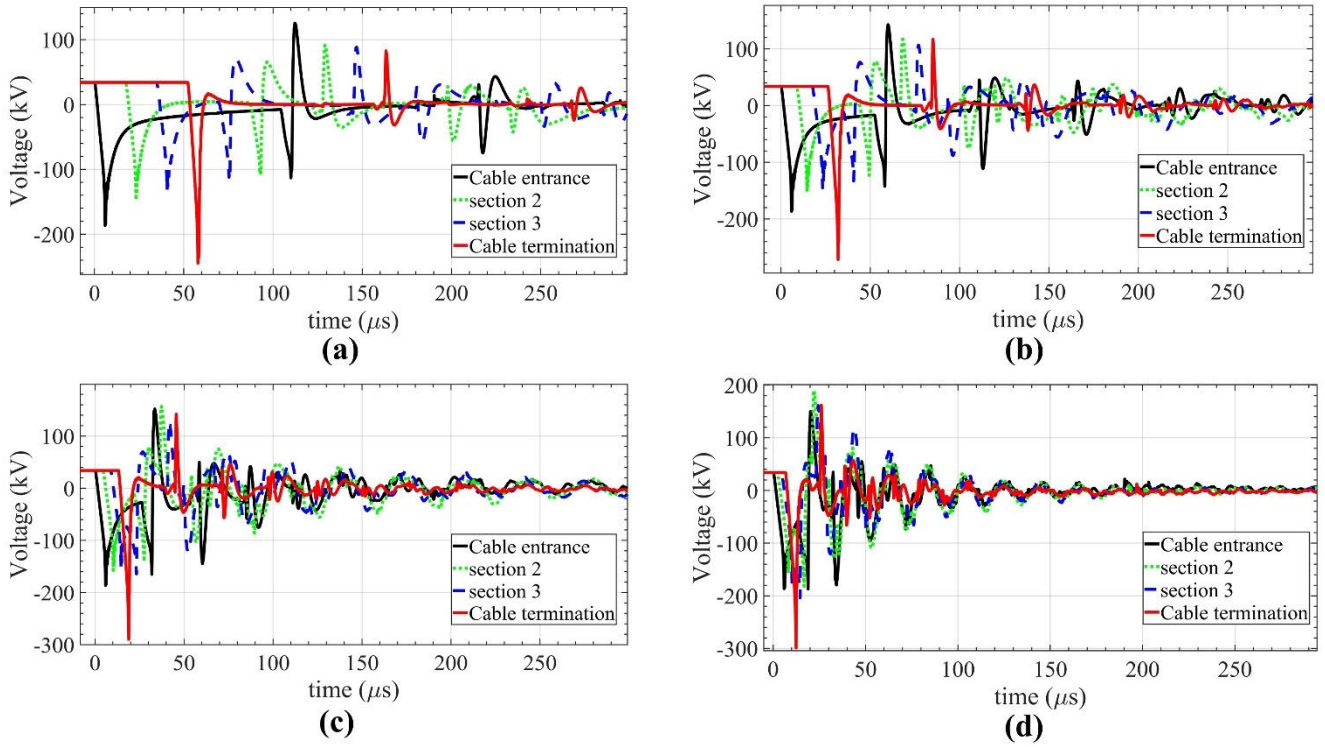

FIGURE 17. Lightning impulse overvoltage at different section for +ve pole underground cable length of (a) 10km (b) 5km (c) 2.5 km (d) 1.25km.

from 10 Ω to 100 Ω. Whereas cable sheath peak overvoltage drastically rises up to 62% (Table. 7).

E. EFFECT OF RISER SURGE IMPEDANCE ON LIGHTNING IMPACT

As described in II-G the riser section surge impedance (Z_{riser}) was taken to be 230Ω for the above considered case. But it can widely vary between overhead transmission surge impedance and cable surge impedance owning to the fact that not much research has been conducted on high-frequency riser section modelling.

Change in riser characteristic impedance cause variation in surge refraction & transmission coefficient which impact $e_f\,(x_r, t)$ and $e_r\,(x_r, t)$. In fig. 18, it can be observed that for tower sections other than T_r, lower riser section surge impedance doesn't account to significant change in disruption coefficient for +ve insulator under 10kA lightning strike. This can be explained based on IV-A, reflections from riser section have lesser impact on flashover of OH tower insulators adjacent to T_r as compared to the steeper portion of lightning surge. Significant increase in disruption coefficient at riser section doesn't cause flashover but may influence the cable overvoltages.

F. INCORPORATION OF SURGE ARRESTERS AND SURGE MITIGATION

Usually, for 35kV insulation lightning-withstand-voltage is about 145 to 170 kV [33]. Recent research papers recommend a higher insulation level for DC cables as compared to AC cable of same voltage [2], [14]. *PSCAD* result show that cable might experience breakdown due to SF or back flashover lightning strikes on OHTL. Thus, an appropriate surge mitigation scheme is required for the cable section. A maximum continuous operating voltage (MCOV) of 39kV is chosen for the surge arrester (1.12 p.u.) [39]. Station low surge arrester (PVI-LP) has been incorporated for the protection of underground cables [40]. The arresters lightning Impulse Protection Level (LIPL) is 148kV while the Switching Impulse Protection level is 105kV. The protection margin (PM) of the arrester can be calculated as:

$$Protection\ margin = \left(\frac{LIWL}{LIPL} - 1\right) \times 100$$

PM is calculated to be 15% for the case under consideration. High-frequency model of a MOSA has been shown in Fig. 19(a) & (b) along with surge arrester's I-V characteristic.

The nonlinear attributes of the surge arrester are represented as A_o and A_1, shown in Fig. 19(a). In case of a slow front (switching impulse), low pass filter in fast front model allows the current to pass through A_1 as well as A_o, manifesting the character of arrester for low-frequency surge. However, in case of a fast front surge only A_1 is suppressed resulting high-frequency response of the arrester. Arrester's V-I characteristic conversion into A_o and A_1 has been performed according to [40] and parameters of single surge arrester model with a height of 0.5842m are evaluated as given in Table. 8.

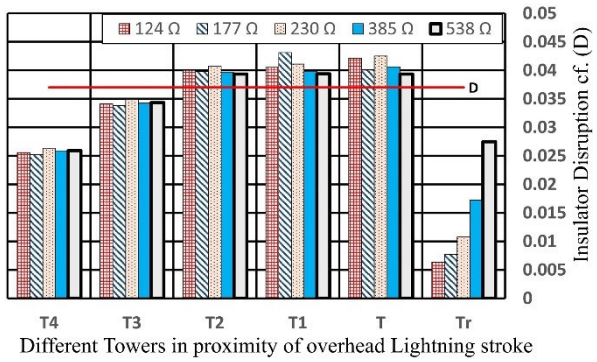

FIGURE 18. Overvoltage Insulation flashover measurement on positive pole with varying riser surge impedance under the influence of I_{MSF}.

On the bases of lightning overvoltage maxima across the cable section. The most vulnerable part i.e., boundaries of the cable, are connected with surge arrester. The resultant forward voltage at the cable entrance $e_f\ (x_{ce}, t)$ as a function of arrester current i_{SA} and initial riser forward voltage $e_f\ (x_{ce}, t)$ can be formulated as (done in [6]):

$$\frac{1}{2}e_{f}\ (x_{ce}, t)\left(1+\frac{Z_{riser}}{Z_{cable}}\right) = e_f\ (x_r, t) - \frac{1}{2}i_{SA}Z_{riser} \quad (21)$$

Equation (21) portrays the influence of cable entrance's arrester on $e_f\ (x_{ce}, t)$. i_{SA} govern the surge overvoltage across the cable. As depicted in Fig. 20 (a), in case of 10kA shielding failure overvoltage impulse is clipped at each portion of the 1.25km long cable. Due to low half-time of I_{MSF} initial overvoltage surge subsides within 50μs. For OHGW lightning (Fig. 20 (b)), this arrester configuration limits the cable overvoltage below LIWL of cable. It is seen that for 1.25m cable surge residual voltage is dictated by lightning wave-shape/half-time and location of surge.

V. LIGHTNING STROKE ON MMC SUBSTATION

Most likely, the converter & substation are heavily protected against any direct lightning strokes. However, lightning overvoltages could traverse through a nearby connected OHTL. To emulate worst-case scenario, lightning fault on tower, 60m away from the converter station is considered.

A. LIGHTNING IMPACT ON SUBSTATION SWITCHGEAR

High-frequency MMC substation modelling (as described in section II-C) suggest that AIS busbar might experience multiple reflection/refraction across it due to difference in characteristic impedance as compared to OHTL and short length (25m). In addition, impact of mutual surge impedance between poles and Earth metallic return have been considered which implies that lightning surge on one pole would also impact the remaining busbars.

Fig. 21 shows the lightning overvoltages waveform across PLD and smoothing reactor in case of 10kA SF current on nearby +ve pole. The initial oscillating voltage surge at pole line disconnector remains till 15μs due to small half-time

TABLE 7. Cable and sheath overvoltages with respect to varying sheath grounding resistance.

Cable Sheath grounding resistance (Ω)	Maximum cable overvoltage (kV)	Maximum sheath Overvoltage (kV)
10	-190	-32.01
25	-197.05	-39.79
50	-200	47.11
75	-202.55	-50.19
100	-203.96	-51.88

TABLE 8. Parameter of surge arrester model.

Components of surge Arrester Model	Magnitude
L_1	4.0017 μH
R_1	37.973 Ω
L_o	0.0068 μH
R_o	58.420 Ω
C_o	171.17 pF

of I_{MSF}. For smoothing reactor, the oscillating surge is low because of its parallel stray capacitance in high-frequency model. Other switchgear equipment like DC circuit breaker, LD, and SD would experience similar overvoltage due to short length and symmetrical modelling in *PSCAD*.

To observe the maximum peak overvoltage, no converter station arrester has been added. As converter station switchgear are interconnected with each other by balancing capacitors & electronic converter structure. The 10kA tower surge also traverses through negative and ground/earth pole switchgear. Fig. 22 shows the response of negative and earth switchgear under the influence of lightning surge at +ve pole.

B. IMPACT OF VOLTAGE SOURCE ON LIGHTNING SURGE AT MMC CONVERTER

In-order to validate the placement of hypothetical voltage source, lightning overvoltages at MMC poles with and without it are needed. Ideally, voltage source across the converter shouldn't alter the voltage waveform at its poles except shifting the surge to nominal voltage of +ve/-ve pole. Fig. 23 shows the lightning voltage waveshape at converter poles under above discussed scenario for 10kA lightning strike. Thus, validating the method to incorporate DC voltage source alongside MMC converter, described in section III-B.

C. LIGHTNING TRANSIENTS ON MMC SUBSTATION DUE TO BF

Low probability OHGW lightning impact is critical to measure the maximum overvoltage that could ever be endured by MMC converter station. 110kA lightning surge is injected into the OHGW adjacent to the substation. The peak overvoltages experience by different converter station sections are illustrated in Fig. 24.

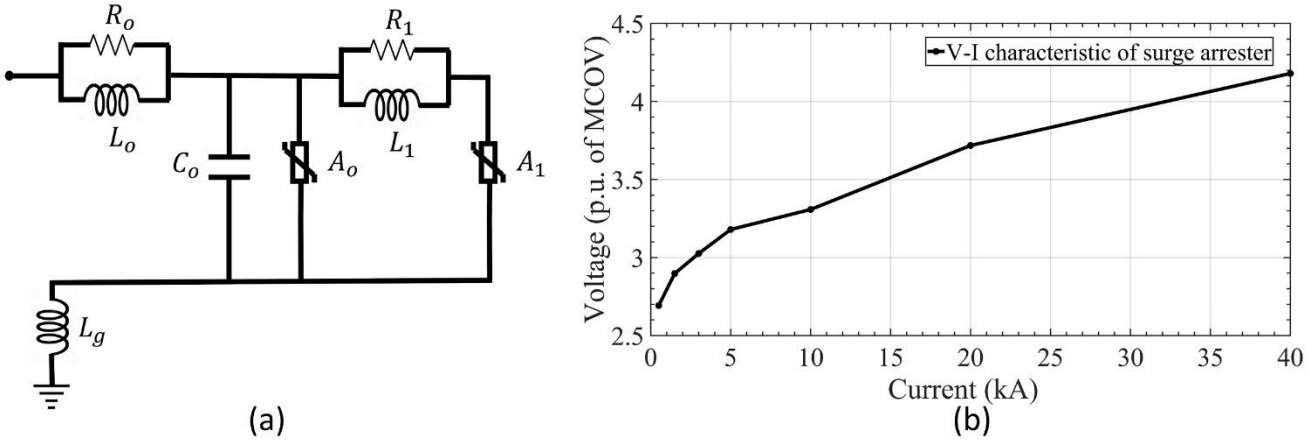

FIGURE 19. (a) fast front model of surge arrester (b) High frequency V-I characteristic of considered PVI-LP SL arrester for 8/20μs lightning waveshape.

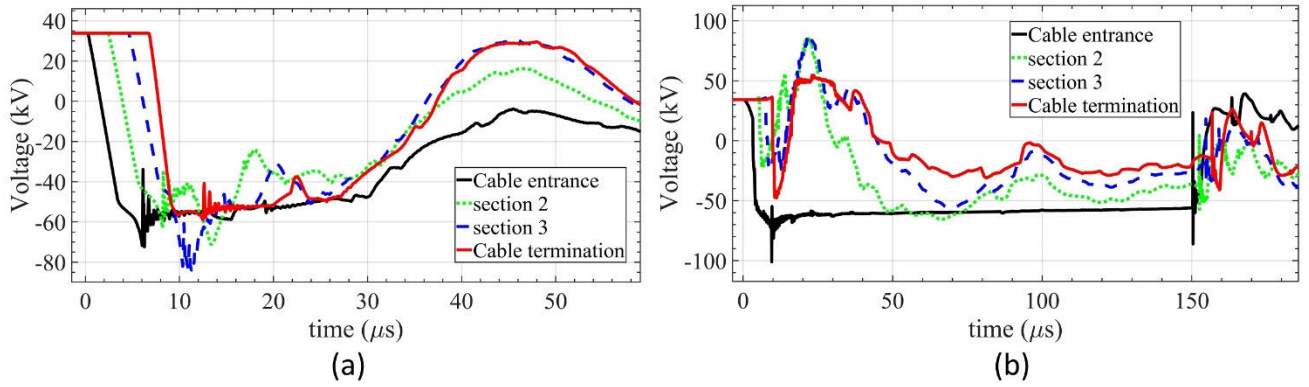

FIGURE 20. Lightning overvoltage at 1.25km long positive cables pole with MOSA (on both ends) due to (a) 10kA MSF (b) 110kA OHGW lightning strike.

D. LIGHTNING SURGE REDUCTION USING ARRESTER AT CONVERTER SWITCHGEAR

It is quite clear that substation peripherals could be damaged due to high magnitude lightning strike or being in close contact to $I_{MSF.}$ To mitigate the risk of insulation damage surge arresters are installed at the switchgear entrance adjacent to tower model in *PSCAD* along with other arresters (i.e. DR) specified in Fig. 5. The resulting voltage waveform at +ve pole disconnector could be noticed in Fig. 25. The peak overvoltage at other converter station portions has been depicted in table. 9. It is tabulated that earthing switchgear still have surge overvoltage above lightning impulse withstand level (170kV) due to direct impact from BF.

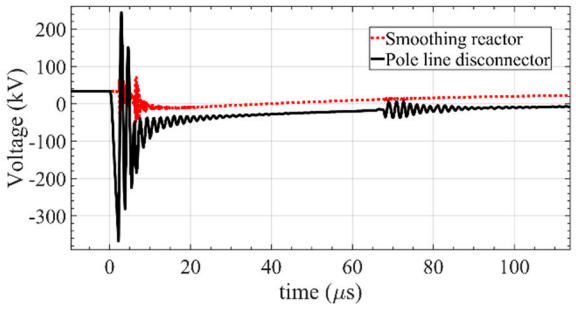

FIGURE 21. I_{MSF} lightning resultant voltages at smoothing reactor and pole line disconnector.

VI. GENERALIZED EVALUATION

To assess the overvoltage surge along an MVDC transmission line, extensive time domain simulation & travelling wave theory based numerical analysis have been carried out and broad range of parameters have been estimated. Following are the assessments regrading main characteristics of MVDC system's lightning behavior:

- SF lightning strike might superimpose a -ve polarity overvoltage surge on positive pole of the tower adjacent to riser/cable section. Flashovers occur at the impacted & adjoining towers' (except the riser tower) +ve insulators, regardless of opposite polarity surge reflections from riser section & underground cables.
- BF on such tower results in insulator breakdown at each of its pole insulators. However, insulator with higher voltage stresses experience flashover first i.e., +ve insulator at the impacted tower experience flashover first due to higher voltage stress from the -ve polarity lightning surge.

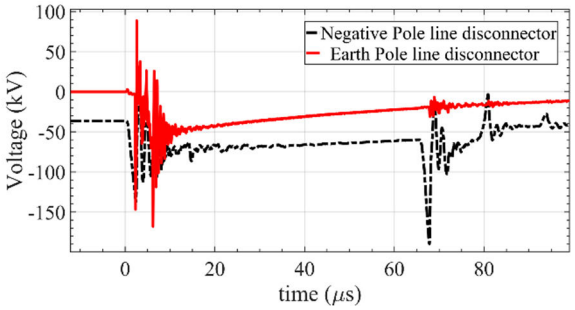

FIGURE 22. Negative and earthing switchgear overvoltage under 10kA lightning surge on nearby positive pole of tower section.

TABLE 9. Lightning peak overvoltage after adding surge arresters at each pole of the substation.

Components of MMC substation	Lightning magnitude (kA)	Peak Voltage (kV)
Positive pole switchgear	10	-80.259
Negative pole switchgear	10	-52.272
Earthing switchgear	10	-70.785
Positive MMC converter terminal	110	-43.54
Negative MMC converter terminal	110	-63.98
Negative pole switchgear	110	-133.94
Earthing switchgear	110	-186.64

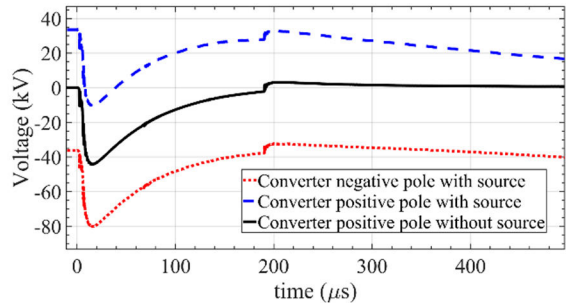

FIGURE 23. 10kA lightning surge response of the converter station poles with and without the hypothetical voltage source.

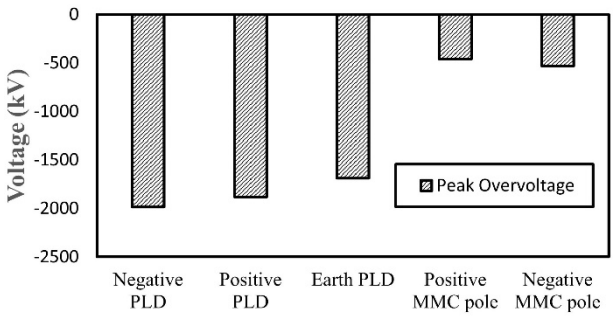

FIGURE 24. 110kA lightning overvoltage maxima at different locations of the converter station without surge arresters.

- In an event of BF on the tower adjacent to riser section, lightning surge on OHGW do not cause immediate back flashover on adjoining towers. This is because part of the surge is retarded by reflection from tower base. However, steeper portion of surge from impacted tower's poles results in flashover of adjoining tower's insulator.
- In case of shielding failure and BF, immediate surge reflections from cable/riser section suppress the flashover of riser pole insulators. However, due to large surge half-time (h_f) of BF lightning, riser tower poles ultimately experience flashover.
- Likeliness of +ve pole insulators at farthest tower increase with higher footing resistance due to SF on tower adjacent to the cable.
- A previous study on mixed HVDC transmission line had shown that riser connected tower is highly resistant to insulator flashover in case of SF/BF lightning incident on it [8]. However, it has been identified in this research that for BF on mixed MVDC transmission line, riser tower poles are prone to insulator flashover. It is expected that installing surge arresters on riser/adjacent tower poles could improve its performance against back flashover lightning.
- Higher riser section characteristic impedance increases the likelihood of insulator disruption at riser tower.
- Without surge arresters at cable joint, it experiences initial surge overvoltage above its Lightning-withstand-level due to shielding failure current at adjacent tower section. Shorter cables tend to have higher terminal overvoltage as well as secondary maxima/minima due to reduction in surge retardation factor and lower propagation time.
- Surge arresters at cable terminal clips the lightning overvoltage across the cable. The surge voltage waveform at cable entrance is dependent on surge arrester current i_{SA}, lightning waveform parameters (S_m& t_h) & transmission/reflection coefficients of cable.
- Lightning surge on MMC substation due to SF on nearby tower's +ve pole results in oscillating overvoltage at impacted busbar pole. Although, overvoltages are observed at -ve pole and earth pole line switchgear but are less severe as compared to the impacted pole switchgear.
- A comprehensive method has been proposed in Section III-B to introduce steady-state system voltage,

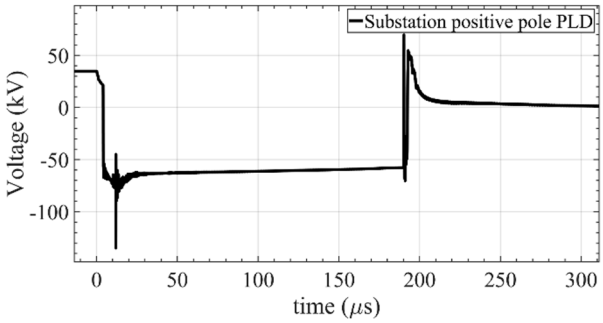

FIGURE 25. 110kA lightning performance of positive line disconnector at the substation.

alongside the MMC converter, in PSCAD simulations for the lightning study of short transmission lines. The validity of this method is demonstrated in V-B by comparing the voltage waveform at the converter poles with and without the hypothetical voltage source. The results show that adding the voltage source shifts the voltage at the converter terminal to the nominal voltage without altering its waveshape.

- Substation without surge arrester show extremely high overvoltage on all poles because of BF on nearby tower. The surge overvoltages are mitigated by surge arresters' configuration across the substation. However, lightning overvoltages still exceed the LIWL at the earth pole switchgear.

Finally, it is emphasized that general lightning impulse levels w.r.t rated system voltage doesn't seem to be a beneficial measure. As they are dictated by project specific parameters i.e. tower structure, grounding condition or cable etc. Additionally, BF resultant overvoltages are estimated for 110kA lightning current amplitude. However, more severe lightning might occur at tower adjacent to cable depending on project specific ground stoke densities, stroke probabilistic nature [36], [37]. Nevertheless, it is deduced that OHGW do not prevent insulator breakdown on impacted towers sections locally in cases of SF/BF. Therefore, in sensitive transitioning regions of MVDC systems where permanent current faults due to lightning strike are need to be avoided, such as OHTL connecting to cables adjacent to a substation, a few adjoining towers should be equipped with both OHGW and tower surge arresters [10].

VII. CONCLUSION

As worldwide number of MVDC projects realized with ''Mixed'' transmission structure rises continuously, a profound understanding of lightning stresses affecting the cable-tower or tower-converter station conjunction are of major importance. This contribution determines the absolute maximum lightning impulse voltage waveforms along the tower section & adjoining underground cable which ranges from 1.25km to 18.75km. Particularly with regards to the lightning surge reflection/refractions from overhead power line, cable and riser section, thorough electromagnetic transient studies have been carried out for backflash over and shielding failure lightning. In addition to that overvoltages at the converter station peripherals have been investigated. Future studies must focus on devising strategies to suppress tower insulator breakdown at critical locations of tower-cable or substation junctions to prevent lightning surge from resulting in current faults. Future discussions need to clarify whether standard lightning impulse test practice should be extended to include superimposed steady-state DC voltages for tower insulators and cables, considering different DC voltage levels. The results obtained within this paper are valuable for insulation coordination of mixed MMC-MVDC transmission system.

APPENDIX

A. ESTIMATION OF MAXIMUM BF OVER OHTL FOR RANGE OF YEARS

Maximum lightning magnitude across the overhead transmission line (OHTL) for a certain period can be evaluated using its back flashover rate (BFR). Highest BFR (flashes/100km/year) for a certain lightning magnitude I, at overhead ground wire directly above tower, is a product of its cumulative probability $P(I)$ and average number of flashes on the OHTL per 100km per year (N_L) [22].

$$BFR = N_L \times P(I) \tag{A.1}$$

By definition, BFR of a single flash of certain lightning current magnitude (I) over a period of Y years on air exposed transmission line of length L (km) can be expressed as:

$$BFR = 1 \Big/ \left(L/_{100} \times Y\right) \tag{A.2}$$

Comparing ($A.1$) & ($A.2$) result in the equation ($A.3$)

$$L/_{100} \times N_L \times P(I) = 1/Y \tag{A.3}$$

Thus, 20km air exposed OHTL experiences a 110kA magnitude lightning strike once in 11.92 or 12 years due to an N_L of 39.624 flash/100km/year.

ACKNOWLEDGMENT

The authors express their gratitude to the Korea Institute of Energy Technology Evaluation and Planning (KETEP).

REFERENCES

[1] S. Coffey, V. Timmers, R. Li, G. Wu, and A. Egea-Àlvarez, ''Review of MVDC applications, technologies, and future prospects,'' *Energies*, vol. 14, no. 24, p. 8294, Dec. 2021, doi: 10.3390/en14248294.

[2] J. Yu, K. Smith, M. Urizarbarrena, N. MacLeod, R. Bryans, and A. Moon, ''Initial designs for the ANGLE DC project; Converting existing AC cable and overhead line into DC operation,'' in *Proc. 13th IET Int. Conf. AC DC Power Transmiss. (ACDC)*, Feb. 2017, pp. 1–6, doi: 10.1049/cp.2017.0002.

[3] *Medium Voltage Direct Current (MVDC) Grid Feasibility Study*, CIGRE Study Committee C6, CIGRE, Paris, France, 2020.

[4] S. Surawijaya, A. A. Buchner, U. Schichler, and S. Harjo, ''Investigation of the possibility to convert medium voltage AC overhead lines (OHL) to DC,'' in *Proc. IEEE 55th Int. Universities Power Eng. Conf. (UPEC)*, Sep. 2020, pp. 1–6, doi: 10.1109/UPEC49904.2020.9209885.

[5] B. Filipović-Grčić, B. Franc, I. H. D. Uglešić, and H. D. Betz, ''Lightning overvoltage protection of combined overhead line and underground cable distribution network,'' in *Proc. CIGRE Int. Colloq. Lightning Power Syst.*, Bologna, Italy, Jun. 2016.

[6] M. Goertz, S. Wenig, C. Hirsching, M. Kahl, M. Suriyah, and T. Leibfried, ''Analysis of extruded HVDC cable systems exposed to lightning strokes,'' *IEEE Trans. Power Del.*, vol. 33, no. 6, pp. 3009–3018, Dec. 2018, doi: 10.1109/TPWRD.2018.2858569.

[7] T. Henriksen, B. Gustavsen, G. Balog, and U. Baur, ''Maximum lightning overvoltage along a cable protected by surge arresters,'' *IEEE Trans. Power Del.*, vol. 20, no. 2, pp. 859–866, Apr. 2005, doi: 10.1109/TPWRD.2005.844262.

[8] M. Asif, H. Lee, U. A. Khan, K. Park, and B. W. Lee, ''Analysis of transient behavior of mixed high voltage DC transmission line under lightning strikes,'' *IEEE Access*, vol. 7, pp. 7194–7205, 2019, doi: 10.1109/ACCESS.2018.2889828.

[9] M. Florkowski, J. Furgał, and M. Kuniewski, ''Lightning impulse overvoltage propagation in HVDC meshed grid,'' *Energies*, vol. 14, no. 11, p. 3047, May 2021, doi: 10.3390/en14113047.

[10] Y. Gao, Y. Han, F. Xiao, C. Chen, J. Zhang, J. Zhang, Y. Zhang, and L. Li, "Study on lightning protection scheme of multi-terminal MMC-MVDC distribution system," *High Voltage*, vol. 5, no. 5, pp. 605–613, Oct. 2020, doi: 10.1049/hve.2019.0256.
[11] W. Z. El-Khatib, J. Holboell, and T. W. Rasmussen, "High frequent modelling of a modular multilevel converter using passive components," in *Proc. Int. Conf. Power Syst. Transients (IPST)*, Vancouver, BC, Canada, Jul. 2013, pp. 1–6.
[12] R. Zhu, N. Lin, V. Dinavahi, and G. Liang, "An accurate and fast method for conducted EMI modeling and simulation of MMC-based HVdc converter station," *IEEE Trans. Power Electron.*, vol. 35, no. 5, pp. 4689–4702, May 2020, doi: 10.1109/TPEL.2019.2945931.
[13] *Compact DC Overhead Lines*, CIGRE Working Group B2.62, CIGRE, Paris, France, 2021.
[14] Y. Liu, X. Cao, and M. Fu, "The upgrading renovation of an existing XLPE cable circuit by conversion of AC line to DC operation," *IEEE Trans. Power Del.*, vol. 32, no. 3, pp. 1321–1328, Jun. 2017, doi: 10.1109/TPWRD.2015.2496178.
[15] *Technical Requirements and Specifications of State-of-the-Art HVDC Switching Equipment*, CIGRE Joint Working Group A3/B4.34, CIGRE, Paris, France, 2017, p. 683.
[16] Y. Han, L. Li, H. Chen, and Y. Lu, "Influence of modeling methods on the calculated lightning surge overvoltages at a UHVDC converter station due to backflashover," *IEEE Trans. Power Del.*, vol. 27, no. 3, pp. 1090–1095, Jul. 2012, doi: 10.1109/TPWRD.2012.2190306.
[17] M. Rioual, "Short and long air gaps (insulator strings and spark gaps) modelling for lightning studies with EMTP program (EPRI-DCG version 2.0)," Tech. Rep., Mar. 1988.
[18] N. Ahmed, L. Ängquist, A. Antonopoulos, L. Harnefors, S. Norrga, and H. Nee, "Performance of the modular multilevel converter with redundant submodules," in *Proc. 41st Annu. Conf. IEEE Ind. Electron. Soc. (IECON)*, Nov. 2015, pp. 3922–3927, doi: 10.1109/IECON.2015.7392712.
[19] U. N. Gnanarathna, A. M. Gole, and R. P. Jayasinghe, "Efficient modeling of modular multilevel HVDC converters (MMC) on electromagnetic transient simulation programs," *IEEE Trans. Power Del.*, vol. 26, no. 1, pp. 316–324, Jan. 2011, doi: 10.1109/TPWRD.2010.2060737.
[20] *ABB HiPak IGBT Module*, ABB Global, Zürich, Switzerland, document 5SNA 1200G450350.
[21] M. Rioual, "Measurements and computer simulation of fast transients through indoor and outdoor substations," *IEEE Trans. Power Del.*, vol. 5, no. 1, pp. 117–123, Jan. 1990, doi: 10.1109/61.107263.
[22] *Guide to Procedures for Estimating the Lightning Performance of Transmission Lines*, CIGRE Working Group 33.01, CIGRE, Paris, France, 1991, p. 63.
[23] Q. Sun, L. Yang, Z. Zheng, J. Han, Y. Wang, and L. Yao, "A comprehensive lightning surge analysis in offshore wind farm," *Electr. Power Syst. Res.*, vol. 211, Oct. 2022, Art. no. 108259, doi: 10.1016/j.epsr.2022.108259.
[24] H. Rao, "Architecture of Nan'ao multi-terminal VSC-HVDC system and its multi-functional control," *CSEE J. Power Energy Syst.*, vol. 1, no. 1, pp. 9–18, Mar. 2015, doi: 10.17775/CSEEJPES.2015.00002.
[25] M. Popov, "Task 6.8 developing a roadmap for VARC DC CB scaling to EHV DC voltage," PROMOTioN, Tech. Rep., 2019, pp. 1–54.
[26] T. Joseph, W. Ming, G. Li, J. Liang, A. Moon, K. Smith, and J. Yu, "Analysis of harmonic transfer through an MVDC link," in *Proc. 15th IET Int. Conf. AC DC Power Transmiss. (ACDC)*, Feb. 2019, pp. 1–6, doi: 10.1049/cp.2019.0017.
[27] W. A. Chisholm, Y. L. Chow, and K. D. Srivastava, "Lightning surge response of transmission towers," *IEEE Trans. Power App. Syst.*, vol. PAS-102, no. 9, pp. 3232–3242, Sep. 1983, doi: 10.1109/TPAS.1983.318134.
[28] L. Grcev, "Modeling of grounding electrodes under lightning currents," *IEEE Trans. Electromagn. Compat.*, vol. 51, no. 3, pp. 559–571, Aug. 2009, doi: 10.1109/TEMC.2009.2025771.
[29] T. Watanabe, K. Fuku, H. Motoyama, and T. Noda, "The measurement and analysis of surge characteristics using miniature model of air insulated substation," in *Proc. Int. Conf. Power Syst. Transients (IPST)*, Jun. 2005, pp. 5–51, doi: 10.3390/en11092492.
[30] *Elektrische Freileitungen; Stützenisolatoren VHD und VHD-G*, Austrian Standard ÖNORM E 4101, 1976.
[31] A. F. Imece, D. W. Durbak, and H. Elahi, "Modeling guidelines for fast front transients," *IEEE Trans. Power Del.*, vol. 11, no. 1, pp. 493–506, Jan. 1996.
[32] R. O. Caldwell and M. Darveniza, "Experimental and analytical studies of the effect of non-standard waveshapes on the impulse strength of external insulation," *IEEE Trans. Power App. Syst.*, vol. PAS-92, no. 4, pp. 1420–1428, Jul. 1973.
[33] *Insulation Co-ordination—Part 1: Definitions, Principles and Rules*, IEC Standard 60071-1, 2006, p. 33.
[34] M. Asif, H.-Y. Lee, K.-H. Park, and B.-W. Lee, "Accurate evaluation of steady-state sheath voltage and current in HVDC cable using electromagnetic transient simulation," *Energies*, vol. 12, no. 21, p. 4161, Oct. 2019, doi: 10.3390/en12214161.
[35] Z. G. Datsios, P. N. Mikropoulos, and T. E. Tsovilis, "Effects of lightning channel equivalent impedance on lightning performance of overhead transmission lines," *IEEE Trans. Electromagn. Compat.*, vol. 61, no. 3, pp. 623–630, Jun. 2019.
[36] *IEEE Guide for improving the Lightning performance of Transmission Line*, IEEE Standard 1243-1997, Dec. 1997.
[37] M. Paolone, R. Farhad, and C. A. Nucci, *IEEE Guide for Improving the Lightning Performance of Electric Power Overhead Distribution Lines*. Piscataway, NJ, USA: IEEE, EPFL Standard 181604, 2010.
[38] ABB Global. *Cables Overvoltage Protection*. Accessed: Jun. 5, 2023. [Online]. Available: https://search.abb.com/library/
[39] *Station Class Surge Arresters IEEE and IEC*. Accessed: Jun. 5, 2023. [Online]. Available: https://hubbellcdn.com/catalogfull
[40] *Metal Oxide Surge Arrester for PSCAD Version 5.0*. Accessed: Jun. 5, 2023. [Online]. Available: https://www.pscad.com/knowledge-base/article/609

MUHAMMAD USMAN was born in Multan, Pakistan, in 1998. He received the bachelor's degree in electrical engineering from the University of Engineering and Technology (UET), Lahore, Pakistan, in 2019. He is currently pursuing the combined M.S. and Ph.D. degree with the HVDC Electric Power Laboratory, Hanyang University, Ansan, South Korea.

His research interests include power electronics, insulation coordination studies for dc grids, protection systems, and switchgear design for HVdc and MVdc systems.

Mr. Usman is a Student Member of the Korean Institute of Electrical Engineers (KIEE) and a member of the Pakistan Engineering Council.

KYU-HOON PARK (Student Member, IEEE) was born in Seoul, South Korea, in 1991. He received the bachelor's degree in electronic system engineering from Hanyang University, Ansan, South Korea, in 2016, where he is currently pursuing the combined M.S. and Ph.D. degree with the HVDC Electric Power Laboratory.

His research interests include power system analysis and protection equipment for dc grids.

Mr. Park is a Student Member of CIGRE and the Korean Institute of Electrical Engineers.

BANG-WOOK LEE (Senior Member, IEEE) received the B.S., M.S., and Ph.D. degrees from the Department of Electrical Engineering, Hanyang University, Seoul, South Korea, in 1991, 1993, and 1998, respectively. He was a Senior Research Engineer with LS Industrial Systems Company Ltd., South Korea. In 2008, he joined the Department of Electronic Engineering, Hanyang University, Ansan, South Korea, where he is currently a Professor. His research interests include HVdc protection systems, high voltage insulation, renewable energies, the development of electrical equipment, and transmission line structures for HVdc and HVac power systems. He is a member of the HVDC Research Committee of KIEE, the Power Cable Experts Committee of the Korean Agency for Technology and Standards, and CIGRE.